Perturbative-polarization-propagator study of the photoionization cross section of the water molecule

Florian Müller-Plathe* and Geerd H. F. Diercksen

Max-Planck-Institut für Physik und Astrophysik, Institut für Astrophysik, Karl-Schwarzschild-Strasse 1, D-8046 Garching bei München, West Germany

(Received 18 January 1989)

Perturbative-polarization-propagator methods of different orders employing large Gaussian basis sets are used to calculate discrete pseudostate representations of the oscillator strength distribution of the water molecule, from which continuous total and partial photoionization cross sections are then determined by moment-theoretical methods. The cross sections obtained in the first-order and second-order polarization-propagator approximation are in very good agreement with recent photoionization measurements. In particular, the present results agree much better with experiment than previous calculations that use the static-exchange approximation. The main reason for this is that first- and higher-order polarization-propagator approximations obey certain sum rules for the oscillator strength distribution, whereas the static-exchange approximation does not. This makes propagator methods particularly well suited for use in connection with moment theory. Disagreement of previously reported cross sections of the water molecule with experiment, such as the overestimation of the $1b_2$ partial cross section, have been partially attributed to the neglect of channel coupling in these calculations. Therefore, in the present work, the separated-channel approximation is avoided and all possible couplings between ionizations from all valence-shell molecular orbitals are allowed for.

I. INTRODUCTION

The importance of water in many environments has stimulated a great deal of investigations of photoprocesses involving the water molecule. More recent experimental studies employing classical and synchrotron radiation sources or, equivalently, fast electrons were aimed at autoionization processes and the rovibrational structure of the resulting ionic states,[1] total,[2,3] and partial[4-10] photoionization cross sections, the electron distribution in the water molecule,[11,12] and the reaction products of dissociative photoionization.[3,4,13]

Theoretical studies of the photoionization of the water molecule have been performed at various levels of approximation. Earlier approaches used plane wave[14] or Coulomb wave[15] expansions for the continuum wave functions. There has also been an attempt to extrapolate molecular photoionization parameters from those of the constituent atoms.[16,17] These methods are computationally very inexpensive, but the resulting cross sections agree only partially with experimental measurements.[2,7] Better agreement with experiment has been obtained by a density-functional (scattered-wave $X\alpha$) calculation.[18] More advanced methods that explicitly construct approximate continuum functions, such as the R-matrix method,[19,20] the linear-algebraic method,[21] or the Schwinger variation procedure,[22,23] have to our knowledge not yet been applied to the water molecule.

The bulk of photoionization cross-section calculations on the water molecule has been carried out using moment-theoretical methods. Moment-theoretical ("Stieltjes imaging") methods (Refs. 24, 25, and refer-

ences therein) have the advantage that they start from a set of discrete transition energies and oscillator strengths which may be calculated by standard quantum-chemical techniques employing finite L^2 basis sets. These discrete transition parameters may, in principle, be calculated at any level of sophistication and, in particular, at any level of electron correlation treatment. Thereby the method allows an easy assessment of the influence of electron correlation on the photoionization cross section.

However, only one of the previous investigations[26] includes electron correlation by means of the time-dependent Hartree-Fock (TDHF) or random-phase approximation (RPA). Unfortunately, the basis set used in that calculation is too small to provide a satisfactory description of the molecular photoionization continuum, and the results are to be taken as qualitative estimates only. The other three moment-theoretical calculations[27-29] employ the static-exchange (SE) approximation and large basis sets for the determination of the discrete pseudostates. They mainly differ in the basis set used. Diercksen et al.[28] used a CGTO (contracted Gaussian-type orbitals) basis set of double-ζ quality augmented by a large number of diffuse functions centered on the oxygen atom. Delaney et al.[27] also used diffuse functions on the hydrogens, allowing for multicenter continuum wave functions. Cacelli et al.[29] used a one-center basis of STO's (Slater-type orbitals) centered on the oxygen that includes hydrogenlike orbitals with appropriate quantum defects for the representation of Rydberg series as well as "oscillating STO's" of the form $r^{n-1}\exp(-\zeta r)\cos kr$ to mimic continuum wave functions. All three basis sets contain nominally around 120 basis functions. However,

as these calculations have been performed in the separated-channel approximation, the actual number of basis functions in the calculations was smaller: for any given ground-state occupied molecular orbital (MO) and transition dipole direction only those diffuse basis functions had to be included that gave rise to nonvanishing transition matrix elements.

The static-exchange approximation has been the most popular approach for the generation of discrete pseudostates for moment-theoretical analyses. It uses a self-consistent field (SCF) description for the molecular ground state. The excited pseudostate wave functions are determined by a singly excited configuration-interaction (SCI) calculation in the space of the SCF canonical virtual orbitals or appropriately modified virtual orbitals. Correlation among the excited pseudostates is introduced through the SCI procedure. However, flexibility is thus given to the excited-states wave functions exclusively and no improvement in the description of the ground state is achieved. Therefore, the static-exchange scheme necessarily leads to an unbalanced approximation in terms of the electron correlation.

An attempt has been made to achieve a better description of the electron correlation in static approaches by including higher than singly excited configurations into the configuration-interaction (CI) expansion.[30,31] This approach though leads quickly to intractable eigenvalue problems, since in the moment-theoretical step of the calculation all energy eigenvalues and transition moments are required and not just the few lowest ones as in bound-state calculations. A further objection to this kind of approach is that limited CI expansions cannot cure the problem of an unbalanced description of the electronic states involved.

Another way to include the influence of electron correlation on the pseudostate properties is the use of linear-response or polarization-propagator (PP) methods. In these approaches it is possible to account for the electron correlation due to higher than singly excited configurations without including these configurations explicitly in the eigenvalue problem. That is to say, the matrix to be diagonalized still has the dimension of the space of all single particle-hole excitations as in the SE approximation. Electron correlation may be included into PP methods in several ways (see below).

In fact, the SE approximation may be viewed as a low-order approximation to the polarization propagator. [To be precise, it falls between zeroth and first order, the zeroth-order approximation being the single-transition approximation (STA).] The first-order PP approximation is equivalent to the TDHF or RPA methods. From the first order upward PP methods have certain invariance properties that static incomplete CI methods do not have, and that make them particularly suitable for use together with moment theory. These invariance properties are described in detail in Sec. III. In spite of the usefulness of RPA there have been only a few applications of this method to photoionization cross-section calculations.[26,32–37] To our knowledge only two moment-theoretical cross-section calculations have been reported to date that treat electron correlation at a higher level

than RPA. One[38] uses a multiconfigurational extension of RPA (MCRPA), the other one[39] uses a PP formulation that is based on a coupled cluster reference state.

In the present contribution a third way of accounting for electron correlation in a PP formulation is pursued. The approach uses as reference state a many-body perturbation theory (MBPT) wave function and evaluates all terms that contribute to the transition energies and oscillator strength consistently through a given order in perturbation theory. In this work the second-order approximation to the PP (SOPPA) is used. The SOPPA method is a well-established technique and there are numerous applications (for a recent account, see Ref. 40). Here it is applied for the first time in a moment-theoretical calculation of photoionization cross sections.

All previous theoretical calculations of the photoionization cross sections of the water molecule have been performed in the separated-channel approximation. This approximation neglects couplings between different ionization channels (ionizations out of different molecular orbitals) and it has been successfully applied to the calculation of partial photoionization cross sections in many cases. However, it has been previously suggested[28] that this approximation is responsible for a significant overestimation of the partial cross section for the $1b_2$ orbital of the water molecule. Furthermore, total cross sections can only be obtained as sums of partial cross sections in this approximation, which leads to discontinuities at each ionization potential. These discontinuities are not found experimentally since channel couplings smoothen the photoionization cross sections in the vicinity of the ionization potentials. Therefore, in this work the couplings between ionizations out of all four valence-shell MO's are investigated.

II. REVIEW OF MOMENT THEORY

The molecular photoionization cross section $\sigma(\omega)$ in megabarns (1 Mb $= 10^{-18}$ cm^2) is proportional to the oscillator strength function $f(\omega)$ in the continuous part of the spectrum

$$\sigma(\omega) = 2\pi^2 \alpha a_0^2 \times 10^{18} f(\omega) \ ,$$

where α is the fine-structure constant and a_0 is the Bohr radius in centimeters. The differential oscillator strength function is given by golden-rule expressions in the dipole-length, mixed dipole-length–dipole-velocity, and dipole-velocity approximation (all quantities in atomic units)

$$f(\omega) = \frac{2}{3} \omega |\langle \Psi(\omega)|\mathbf{r}|0\rangle|^2 \ ,$$

$$f(\omega) = i\frac{2}{3} \langle 0|\mathbf{r}|\Psi(\omega)\rangle \langle \Psi(\omega)|\mathbf{p}|0\rangle \ ,$$

$$f(\omega) = \frac{2}{3} \frac{1}{\omega} |\langle \Psi(\omega)|\mathbf{p}|0\rangle|^2 \ ,$$

where $|0\rangle$ is the electronic ground state with the energy E_0, $\Psi(\omega)$ is a continuum state with energy $E_0 + \omega$, and $\mathbf{r}$ and $\mathbf{p}$ are the electron position and momentum operator, respectively. These expressions correspond to the more

familiar ones for excitations to discrete states $|i\rangle$

$$f_i = \frac{2}{3}\omega_i |\langle i|\mathbf{r}|0\rangle|^2 ,$$

$$f_i = i\frac{2}{3}\langle 0|\mathbf{r}|i\rangle\langle i|\mathbf{p}|0\rangle ,$$

$$f_i = \frac{2}{3}\frac{1}{\omega_i}|\langle i|\mathbf{p}|0\rangle|^2 .$$

The three formulations become equivalent when $|0\rangle$ and $\Psi(\omega)$ or $|i\rangle$ are either exact solutions of the electronic Schrödinger equation or if they are calculated within certain models (see Sec. III).

The continuous oscillator strength cannot be calculated directly in a discrete basis set since the L^2 basis discretizes the continuous spectrum of the electronic Hamiltonian. However, $f(\omega)$ may be calculated from its power moments $S(k)$

$$S(k) = \int_{\omega_T}^{\infty} \omega^k f(\omega)d\omega ,$$

where ω_T is the appropriate ionization threshold. Negative moments are used throughout this work because of the well-known divergence of the moments with $k > 2$.[41,42] If all moments are known (which means an infinite number of moments) $f(\omega)$ is determined completely. However, in practice only a limited number of moments may be calculated with reasonable accuracy from a set of discrete transition energies $\bar{\omega}_i$ and oscillator strength $\bar{f}_i$

$$S(-k) \approx \sum_{i=1}^{N} (1/\bar{\omega}_i)^k \bar{f}_i , \quad k = 0, 1, \ldots, 2n-1 .$$

The sum extends over all N transitions with $\bar{\omega}_i > \omega_T$, and $n > 0$ is usually much smaller than N. Therefore, $f(\omega)$ is not completely determined, i.e., there may be more than one function whose moments are equal to $S(0), S(-1), \ldots, S(-2n+1)$.

Given a finite number of moments it is, however, possible to find an nth-order approximation $f^{(n)}(\omega)$ to $f(\omega)$ in such a way that consecutive orders converge to $f(\omega)$ in the limit of large n. This convergence is ensured by the Chebyshev inequalities.[43] The algorithm for finding $f^{(n)}(\omega)$, the so-called Stieltjes method, as implemented in the program SCAMPI (Stieltjes-Chebyshev analysis of molecular photoionization[44]) is briefly described in the following.

From the discrete transition parameters $\bar{\omega}_i$ and $\bar{f}_i$ a new set of n transition energies ω_i and oscillator strengths f_i is determined which reproduce the first $2n$ approximate moments

$$S(-k) = \sum_{i=1}^{n} (1/\omega_i)^k f_i , \quad k = 0, 1, \ldots, 2n-1 .$$

The $1/\omega_i$ and f_i may also be viewed as quadrature abscissas and weights for a generalized Gaussian quadrature rule associated with the density or weight function $f(\omega)$ and the integration interval from ω_T to infinity.[45] They are calculated from the orthogonal polynomial $Q_n(1/\omega)$

$$\int_{\omega_T}^{\infty} Q_n(1/\omega)Q_m(1/\omega)f(\omega)d\omega = N_n\delta_{nm} ,$$

where $N_n = \int_{\omega_T}^{\infty} Q_n^2(1/\omega)f(\omega)d\omega$. The $1/\omega_i$ can be ob-

tained as the n roots of $Q_n(1/\omega)$

$$Q_n(1/\omega_i) = 0$$

and the f_i may be calculated from

$$f_i = \left[\sum_{m=0}^{n-1} \frac{Q_m^2(1/\omega_i)}{N_m} \right]^{-1} .$$

In this work a faster numerical method is used that obtains the ω_i and f_i from the eigenvalues and eigenvectors of a tridiagonal symmetric matrix.[45,46]

The orthogonal polynomials are generated recursively by an algorithm originally proposed by Chebyshev[45,47]

$$Q_0(1/\bar{\omega}_i) = 1 ,$$

$$a_1 = \sum_{i=1}^{N} (1/\bar{\omega}_i)\bar{f}_i \Big/ \sum_{i=1}^{N} \bar{f}_i ,$$

$$Q_1(1/\bar{\omega}_i) = (1/\bar{\omega}_i) - a_1 ,$$

$$b_{n-1} = \frac{1}{b_0 b_1 \cdots b_{n-2}} \sum_{i=1}^{N} (1/\bar{\omega}_i)^{n-1}Q_{n-1}(1/\bar{\omega}_i)\bar{f}_i ,$$

$$a_n = \frac{1}{b_0 b_1 \cdots b_{n-1}} \sum_{i=1}^{N} (1/\bar{\omega}_i)^n Q_{n-1}(1/\bar{\omega}_i)\bar{f}_i - \sum_{l=1}^{n-1} a_l ,$$

$$Q_n(1/\bar{\omega}_i) = [(1/\bar{\omega}_i) - a_n]Q_{n-1}(1/\bar{\omega}_i)$$
$$- b_{n-1}Q_{n-2}(1/\bar{\omega}_i) .$$

This algorithm can be shown[44] to be equivalent to the one given by Langhoff et al.[48] In this recurrence algorithm the approximate moments do not appear explicitly but are hidden in the summations over all discrete transitions, so that the success of this method still depends on the ability of the discrete transitions from an L^2 calculation to reproduce the moments of $f(\omega)$ with sufficient accuracy. Moreover, although this direct recurrence algorithm based on the $\bar{\omega}_i$ and $\bar{f}_i$ seems to be numerically more stable than a recurrence starting from the $S(k)$,[48] it should be noted that because of the differencing involved in each step all orthogonal polynomial recurrence algorithms become unstable for large n. To avoid numerical problems this part of the calculation is carried out in 128-bit precision.

Given the ω_i and f_i an nth-order approximate distribution function $F^{(n)}(\omega)$ is then constructed

$$F^{(n)}(\omega) = \begin{cases} 0, & \omega < \omega_1 \\ \sum_{j=1}^{i} f_j, & \omega_i < \omega < \omega_{i+1} \\ \sum_{j=1}^{n} f_j = S(0), & \omega_n < \omega \end{cases}$$

which is a nondecreasing "staircaselike" function and which approximates the cumulative oscillator strength

$$F(\omega) = \int_{\omega_T}^{\omega} f(\omega')d\omega' .$$

Numerical differentiation of $F^{(n)}(\omega)$ yields the desired nth-order approximant $f^{(n)}(\omega)$

$$f^{(n)}(\omega) = \frac{1}{2}\frac{f_1}{\omega_1}, \quad \omega < \omega_1$$

$$f^{(n)}(\omega) = \frac{1}{2}\frac{f_{i+1}+f_i}{\omega_{i+1}-\omega_i}, \quad \omega_i \leq \omega < \omega_{i+1}$$

$$f^{(n)}(\omega) = 0, \quad \omega_n < \omega .$$

In order to obtain a continuous nth-order approximation these data points are interpolated by a cubic spline function. A monotonicity-constrained spline[49] has been found particularly useful since it follows the original data very closely and avoids overshooting.

As an alternative approach to continuous oscillator strength functions the use of the so-called Chebyshev procedure has been proposed.[24,25] It is closely related to the Stieltjes procedure, except that it allows one of the quadrature abscissas ω_i, say ω_0, to be varied at will over the energy range. This is done by replacing the orthogonal polynomial $Q_n(1/\omega)$ of the Stieltjes development by the quasiorthogonal polynomial $q_n(1/\omega)$

$$q_n(1/\omega) = Q_n(1/\omega) - \tau Q_{n-1}(1/\omega) ,$$

where $\tau = Q_n(1/\omega_0)/Q_{n-1}(1/\omega_0)$. This polynomial is orthogonal to all $Q_m(1/\omega)$ with $m \leq n-2$ but not to $Q_{n-1}(1/\omega)$, and it may be generated by the modified recurrence relation

$$q_n(1/\omega) = [(1/\omega) - a_n - \tau]Q_{n-1}(1/\omega)$$
$$- b_{n-1}Q_{n-2}(1/\omega) .$$

Note that only the polynomial of degree n has changed, the polynomials of lower degrees being the same as in the Stieltjes case. Again, the quadrature abscissas and weights may be calculated from

$$q_n(1/\omega_i) = 0 ,$$

$$f_i = \left[\sum_{m=0}^{n-1} \frac{Q_m^2(1/\omega_i)}{N_m} \right]^{-1} .$$

Since ω_0 may be varied continuously, a continuous approximate distribution function $F^{(n)}(\omega)$ can be obtained which may be differentiated analytically to yield the desired continuous approximate density $f^{(n)}(\omega)$. The exact formulas for the derivative have been given by Corcoran and Langhoff[24] (beware of misprints).

The Chebyshev approach seemingly is an attractive alternative to spline interpolation of the Stieltjes density. However, there are several problems associated with it. Firstly, its quadrature abscissas and weights render an exact quadrature only for polynomials of degree up to $2n-2$ instead of $2n-1$ as required for an nth-order Gaussian quadrature. Therefore, the "nth-order" Chebyshev distribution and density are not strictly of order n but fall between the true nth and the true $(n-1)$th order. Secondly, it has been observed previously[24] that one of the Chebyshev abscissas may fall below ω_T. This is a consequence of the fact that one of the roots of any quasiorthogonal polynomial is not confined to lie in the interval of orthogonality between ω_T and infinity as opposed to the roots of orthogonal polynomials. The theory of quasiorthogonal polynomials predicts in more detail under which circumstances, that is to say for which choice of τ, one root escapes from the interval of orthogonality.[43,50] Here, it is merely noted that in the application to photoionization τ has to be less than

$$Q_n(1/\omega_0)/Q_{n-1}(1/\omega_0)$$

for all ω_i to lie above ω_T. This implies that certain values of τ and, in consequence, certain values of ω_0 may not be used if unphysical results are to be avoided.

The most severe drawback of the Chebyshev method, however, arises from the fact that in contrast to the orthogonal polynomials there is nothing that prevents a quasiorthogonal polynomial to run almost parallel to the abscissa in the vicinity of a root. This is the case when its first derivative (and possibly higher derivatives) are numerically zero around the root $(1/\omega_i)$

$$0 \approx q_n'(1/\omega_i) \approx q_n''(1/\omega_i) \approx \cdots$$

which occurs if

$$\tau \approx \frac{Q_n'(1/\omega_i)}{Q_{n-1}'(1/\omega_i)} \approx \frac{Q_n''(1/\omega_i)}{Q_{n-1}''(1/\omega_i)} \approx \cdots ,$$

As a result it becomes very difficult for any numerical root search algorithm to locate $1/\omega_i$ accurately. Instead, it may find a point in the vicinity where $q_n(1/\omega)$ is also numerically very small. This numerical instability causes parts of the energy range to become repulsive for roots, i.e., if an attempt is made to place ω_0 into such a region, then ω_0 is not recovered by the root search method but it is "pushed" to one edge of that region. Similar problems with the Chebyshev procedure have also been observed elsewhere.[51] Implementation in higher precision arithmetic does not avoid these artifacts sufficiently. A numerically much more robust way of obtaining continuous approximate cross sections is the aforementioned spline interpolation.

III. OSCILLATOR STRENGTH SUM RULES

As described in the previous section the moments $S(k)$ of the oscillator strength density function $f(\omega)$ in the continuous part of the spectrum enter the moment-theoretical calculation of the photoionization cross section either directly or implicitly. Accurate calculation of the $S(k)$ by the discrete transition energies and oscillator strengths from an L^2 calculation is essential for the moment-theory approach to be successful. It would therefore be desirable to compare the calculated $S(k)$ directly to experimentally measured $S(k)$. These may, in principle, be determined by appropriate integrations of the experimental photoionization cross sections. Unfortunately, for many molecules the cross sections are not available in the complete energy range or are too inaccurate.

In contrast, several of the total oscillator strength moments $s(k)$

$$s(k) = \sum_{\text{discr}} \omega_i^k f_i + \int_{\text{cont}} \omega^k f(\omega) d\omega$$

that include excitations to discrete states as well as ionization, are related by sum rules to physical observables or to expectation values of certain operators over the ground-state wave function $|0\rangle$,[41,42,52]

$$s(-2) = \bar{\alpha} ,$$

$$s(-1) = \frac{2}{3}\left\langle 0 \left| \left[\sum_{i=1}^{N} \mathbf{r}_i \right]^2 \right| 0 \right\rangle ,$$

$$s(0) = N ,$$

$$s(1) = \frac{2}{3}\left\langle 0 \left| \left[\sum_{i=1}^{N} \mathbf{p}_i \right]^2 \right| 0 \right\rangle ,$$

$$s(2) = \frac{4}{3}\pi N \left\langle 0 \left| \left[\sum_{i=1}^{N} \delta(\mathbf{r}_i) \right]^2 \right| 0 \right\rangle .$$

Here, N denotes the number of electrons in the molecule, $\bar{\alpha}$ the average static electric dipole polarizability, $\mathbf{r}_i$ and $\mathbf{p}_i$ the position and momentum operators of electron i, and all quantities are in atomic units. Note that the sum rules apply to the exact wave functions as well as to certain approximations, provided that the basis-set error is eliminated. Of these sum rules, $s(-2)$ and $s(0)$ are particularly important in the present context. The Thomas-Reiche-Kuhn (TRK) sum rule $s(0)$ normalizes the oscillator strength distribution, so that it must be obeyed by the L^2 calculation in order to avoid global overestimation or underestimation of the cross section. The dipole polarizability is the highest negative moment that can be measured conveniently. If the polarizability is not reproduced, it is very likely that the higher negative moments are incorrect as well.

Closely related to the normal sum rules are the logarithmic sum rules $l(k)$

$$l(k) = \sum_{\text{discr}} \omega_i^k \ln(\omega_i) f_i + \int_{\text{cont}} \omega^k \ln(\omega) f(\omega) d\omega .$$

The $l(k)$ and $s(k)$ define the set of so-called mean excitation energies $I(k)$

$$I(k) = \exp\left[\frac{l(k)}{s(k)} \right]$$

which appear in the Bethe treatment of charged-particle impact on matter:[53–55] $I(-1)$ is related to the cross section for electron excitation or ionization, $I(0)$ to the energy deposition (stopping power), and $I(1)$ to its mean fluctuation or straggling. The Lamb shift of electronic energy levels is governed by $I(2)$.[42]

Different sum rules depend on different parts of the oscillator strength distribution: in the case of H_2O for example, 97% of the oscillator strength lies above the first ionization threshold of 12.61 eV,[3] so that the discrete part contributes only 3% to the TRK sum rule. On the other hand, this part contributes 25% of the polarizability.[3] Consequently, the calculation of different sum rules encompasses different computational problems. For the TRK sum rule a balanced description of the whole spectrum, including the high-energy continuum, is important. In contrast, the polarizability is completely determined by the discrete excitations and the low-energy continuum. For example, the continuum above 100 eV contributes less than 0.1% to the polarizability of H_2O. On the other hand, $\bar{\alpha}$ (and the higher negative moments even more) depends on a few low-energy excitations and ionizations which must be calculated very accurately. These sums rules become especially sensitive to the small excitation energies because they enter with inverse powers. For moments or mean excitation energies that contain positive powers or functions of ω the opposite is true. They depend mainly on the high-energy continuum part of the spectrum. Therefore, this part must be well described in order to reproduce for example $I(0)$ correctly.

IV. POLARIZATION-PROPAGATOR METHODS

The theory of polarization-propagator techniques is covered in detail by a number of review articles.[40,56–58] Here, only the aspects of PP theory relevant to moment-theoretical calculations are briefly summarized.

Linear-response theory deals with the response of a system to an external perturbation. In the case of the PP the perturbation may be a time-dependent electric field in which case the propagator yields information about electric dipole transitions. In contrast to the more familiar static approaches linear-response theory avoids the calculation of ground-state and excited-states wave functions, but obtains the transition energies and oscillator strength directly from the poles and residues of the PP.

The lowest-order PP approximation is equivalent to a CI calculation that includes all single excitations. This method is also known as the multichannel static-exchange (SE) approximation or Tamm-Dancoff approximation. It has in common with all incomplete CI expansions that oscillator strengths obtained in the dipole-length and dipole-velocity formulations are generally different, even for a complete basis set. The transition energies and oscillator strengths obtained in the SE approximation do not satisfy any of the sum rules of Sec. III.

The first-order PP approximation (RPA or TDHF) differs from the SE approximation in that the SCF determinant is no longer used as the electronic ground state but merely as a reference state for the generation of the first-order PP matrix or RPA matrix. The manifold of excitation operators now includes all single excitations and deexcitations. This leads to elements in the RPA matrix that correspond to double substitutions in addition to the singly excited terms that are already present in the SE matrix. Provided the basis set is large enough and all possible single particle-hole excitations are included, the different formulations for the oscillator strengths are completely equivalent in RPA, and the TRK sum rule is obeyed exactly. Note that the basis set need not include continuum functions for the TRK sum rule to be satisfied. A discrete L^2 basis, if sufficiently large, recovers all of the continuum oscillator strength. The RPA static electric dipole polarizability and other second-order response properties are equal to these properties obtained in the coupled Hartree-Fock (CHF) approximation within the same basis set. As the RPA oscillator strengths are identical in different dipole gauges, all oscil-

lator strength moments become identical as well.

It has been noted previously that often more reliable results can be obtained in the SE approximation if the mixed length-velocity gauge is used.[36,37] This feature is not due to the inclusion of electron correlation effects[59] in this gauge at the SE level as has been claimed,[36] but rather to cancellations of errors. It can be shown[60] that the TRK sum rule calculated in the mixed gauge must be equal in the zeroth- and first-order PP approximations, and in fact also in higher-order perturbative PP approximations. This equivalence holds only for $s(0)$, the transition energies obtained in different orders are considerably different, so that other moments than $s(0)$ differ as well.

Of the linear-response methods that go beyond the RPA level, only MCRPA provides a strict dipole-length–dipole-velocity equivalence and only MCRPA obeys the TRK sum rule exactly in all gauges. The reason for this is that only RPA, MCRPA and a hypothetical full-CI PP satisfy the time-dependent analog of the Hellmann-Feynman theorem.[61] For the perturbative PP applied in the present work Jørgensen and Oddershede[62] have shown that the equivalence restrictions and the sum rules are fulfilled through the order in perturbation theory through which the PP is evaluated consistently. This is in marked contrast to the SE approximation which may produce large differences between oscillator strengths calculated in different gauges and errors in the TRK sum rule often of the order of 25% or more.

The second-order PP approximation that is employed in the present work uses as the reference state an MBPT expansion which contains double substitutions in first order and single substitutions in second order. All elements of the PP matrix and all contributions to the transition moments are evaluated consistently through second order in perturbation theory so that transition energies and oscillator strengths are consistent through second order. To achieve a consistent second-order treatment terms involving singly, doubly, and triply substituted configurations have to be included implicitly into the SOPPA method.[63]

V. COMPUTATIONAL DETAILS

The calculations of the photoionization cross sections and of the oscillator strength sum rules are performed in the vertical approximation at the experimental equilibrium geometry of the water molecule [$R(OH) = 1.811096$ a.u., $\alpha = 104.4499°$ (Ref. 64)]. In all calculations the Cartesian coordinate origin is placed at the molecular center of mass.

Special attention must be paid to the selection of the basis set (see Table I). In the foregoing sections it has been emphasized that the discrete basis set must sample the entire spectral range equally well for all oscillator strength sum rules to be obeyed and hence for the discrete transition energies and oscillator strengths to be useful in the moment-theoretical analysis. More specifically, there are three requirements on the basis set: (i) The basis must describe the molecular ground state sufficiently well, a condition which is easily met by many

extended basis sets. (ii) The basis must span the bound excited states, including a number of Rydbeg states, as well as the low-energy ionization continuum. This region of the spectrum is important for a correct reproduction of the higher negative moments. This is generally achieved by adding a large number of diffuse functions to the basis whose exponents continue the geometric progression of those of the valence basis. Requirements (i) and (ii) have been used as guidelines for the choices of the basis sets used in two of the previous photoionization cross section calculations of water.[27,28] (iii) More recently, however, it has been realized that for a reliable reproduction of the lower negative moments, and especially the TRK sum rule, sufficient flexibility of the basis set in the high-energy continuum is essential. In the case of the water molecule 26.2% of the cumulative oscillator strength is contributed by the region above 125 eV.[2] The continuum functions at high energies are very contracted and show rapid oscillations in the molecular region. An effective way of mimicking this behavior is to select an in-

TABLE I. Exponents of uncontracted Cartesian Gaussian basis sets used in this work.

	Oxygen		Hydrogen
	Basis set 101[a]	Basis set 105[b]	
	s functions		
1	105 374.945 3200	15 679.240 3310	1776.776 559
2	15 679.240 3310	3534.544 6760	254.017 712
3	3534.544 6760	987.365 1600	54.698 039
4	987.365 1600	315.978 7520	15.018 344
5	315.978 7520	111.654 2810	4.915 078
6	111.654 2810	42.699 4510	1.794 924
7	42.699 4510	17.395 5960	0.710 716
8	17.395 5960	7.438 3090	0.304 802
9	7.438 3090	3.222 8620	0.138 046
10	3.222 8620	1.253 8770	0.062 157
11	1.253 8770	0.495 1550	
12	0.495 1550	0.191 6650	
13	0.191 6650	0.076 6660	
14	0.076 6660	0.030 6664	
15	0.030 6664	0.012 0000	
16		0.005 0000	
	p functions		
1	200.000 0000	46.533 3670	1.500 000
2	46.533 3670	14.621 8090	0.400 000
3	14.621 8090	5.313 0640	0.100 000
4	5.313 0640	2.102 5250	
5	2.102 5250	0.850 2230	
6	0.850 2230	0.337 5970	
7	0.337 5970	0.128 8920	
8	0.128 8920	0.046 0000	
9		0.017 0000	
	d functions		
1	4.000 0000	1.218 8700	
2	1.218 8700	0.361 0200	
3	0.361 0200	0.100 0000	
4	0.100 0000	0.030 0000	

[a]418 dipole-allowed transitions.
[b]436 dipole-allowed transitions.

itial basis set that contains functions with large exponents and leave this basis completely uncontracted.

These considerations lead to the choice of a (15.8.4./10.3.) uncontracted GTO basis set of 101 functions (denoted as basis set 101 in Table I). It has been optimized by Lazzeretti and Zanasi[64] to reproduce the TRK sum rule at the RPA level. It has also been used successfully for the calculation of mean excitation energies.[65] In order to check the relative importance of very compact and very diffuse basis set functions an uncontracted (16.9.4./10.3.) GTO basis set consisting of 105 functions (basis set 105) is derived from basis set 101 by deleting the most compact s, p, and d functions on the oxygen atom and adding two more sets of diffuse s and p functions and one more set of diffuse d functions (Table I). Although these bases are optimized for sum rules and not for total energies the SCF total and orbital energies are very close to their Hartree-Fock limit values as can be seen by comparison with the best available SCF calculation on H_2O that included 140 CGTO functions[12] (see Table II). A comparison with an SCF calculation that includes all basis-set functions that appear in basis set 101 and/or basis set 105 (denoted as basis set 115) indicates that omitting the innermost s function in going from basis set 101 to basis set 105 accounts for most of the energy difference. The addition of the very diffuse functions to basis set 101 has a negligible effect on the total and orbital energies which suggests that the bases are almost complete in this region.

Calculation of the discrete transition energies and oscillator strengths is performed with the perturbative polarization propagator program for closed-shell reference states[66] which is part of the MUNICH program system.[67] The SE and first-order (RPA) calculations are generally performed including all excitations possible within the the given basis set. Due to the large disk space requirements in the present implementation the excitation space has to be truncated in second-order (SOPPA) calculations. The lowest occupied orbital which corresponds to an inner-shell oxygen $1s$ orbital can safely be excluded since no mixing between inner-shell and valence-shell excitations occurs at the SE and RPA levels. The virtual space is truncated so that there are 60–65 single particle-hole transitions per polarization direction left to be treated in SOPPA. These cover the photon energy range from 0 to approximately 90 eV, which dominates the higher negative moments. The remaining spectrum is filled in with the transitions from a complete RPA calculation.

This splitting is only necessary in the calculation of the sum rules and the total photoionization cross sections where coupling between all valence channels is allowed for.

The partial cross sections reported in this contribution are calculated in the separated-channel approximation: only excitations from the one occupied orbital which forms the ionization channel under consideration are included in the calculation. This reduces the number of single particle-hole excitations so that the whole virtual orbital space can be included at all orders, including SOPPA. The same orbital space is used for both the generation of the particle-hole excitations and the treatment of electron correlation within the chosen order of perturbation theory.[57,66] All propagator matrix elements prescribed by the perturbation scheme are evaluated in this restricted space. In SOPPA, for instance, there are contributions from two-hole–two-particle excitations which are not contained in RPA (for explicit formulas for the matrix elements in different orders, see Ref. 57).

VI. SUM RULES OF THE WATER MOLECULE

Calculations of the total oscillator strength distribution moments $s(k)$ from the discrete transition energies and oscillator strengths and comparison to theoretical or experimental reference data provides a check on the quality of the L^2 oscillator strength. The moments $s(0)$, $s(-1)$, $s(-2)$, and $27.211[I(0)]$ (in eV) calculated in the zeroth-, first-, and second-order polarization propagator approximation are listed in Tables III–VI, respectively, together with theoretical and experimental reference values, if available.

The quality of the reference data varies considerably among the moments. There is no ambiguity for the TRK sum rule. The static dipole polarizability has been determined very accurately both by experiment (Raman spectroscopy[68]) and theory. Here the SDTQ-MBPT(4) (fourth-order MBPT including all single, double, triple, and quadruple substitutions) values of Ref. 69 are given; for an account of other recent calculations of the polarizability of water see Ref. 44). The values of the other two moments are less certain. There is a considerable scatter among the experimental data for $s(-1)$, and $I(0)$ cannot be determined directly by experiment.

Comparison of all calculated moments with the reference data clearly shows that the static-exchange approximation fails to reproduce the oscillator strength distribu-

TABLE II. SCF total and orbital energies for the water molecule (in a.u.).

	Basis set 101	Basis set 105	Basis set 115	140 GGTO basis set[a]	Expt.[b]
$1a_1$	−20.564 581	−20.565 555	−20.564 731		−19.83
$2a_1$	−1.352 418	−1.352 967	−1.352 526		−1.18
$1b_2$	−0.717 962	−0.717 988	−0.718 069		−0.6802
$3a_1$	−0.585 296	−0.585 119	−0.585 405		−0.5417
$1b_1$	−0.509 064	−0.509 092	−0.509 114		−0.4638
Total energy	−76.065 283	−76.063 184	−76.065 304	−76.0673	

[a]Reference 12.
[b]References 71 and 72.

TABLE III. TRK sum rule $s(0)$ for the water molecule in the dipole-length (DL), dipole-velocity (DV), and mixed (DL-DV) approximation.

	DL	DV	DL-DV
Basis set 101			
SE	12.08	8.42	9.97
RPA	10.19	9.78	9.97
SOPPA	10.13	9.89	10.00
Basis set 105			
SE	11.94	8.25	9.81
RPA	9.90	9.73	9.81
SOPPA	10.04	9.73	9.88
Theory			
RPA[a]	10.0065	9.9450	
Exact	10		
Experiment			
Photoabsorption[b]	9.99		
EMS[b]	10.02		
Photoabsorption and EMS[c]	10.00		

[a]References 64 and 65.
[b]Reference 3.
[c]Reference 2.

tion of the water molecule. Moreover, it is clearly seen that the disagreement of the dipole-length and the dipole-velocity approximation within SE is considerable, while the moments in the mixed approximation equal those in the mixed approximation in RPA as predicted by theory. Because of the inability of SE to reproduce correctly the known moments its use together with moment-theoretical methods does not seem justified, given that more appropriate methods are available.

The TRK sum rule in the random-phase approximation approaches very closely the exact value of 10, and the RPA polarizability is equal to a CHF polarizability obtained using a specially optimized basis set.[69] The agreement of the RPA moments calculated in different gauges is very good. The moments calculated in different gauges in the second-order approximation show a slightly larger spread than the corresponding RPA values, as is expected from theory. However, these deviations are much smaller than those of the SE values. The SOPPA moments are generally closer to experiment than the RPA moments. The convergence with the order of the MBPT expansion, however, does not seem to be uniform in all cases. In particular, the dipole polarizability of the water molecule is underestimated by RPA while it is

TABLE IV. Moment $s(-1)$ for the water molecule in the dipole-length (DL), dipole-velocity (DV), and mixed (DL-DV) approximation (in a.u.).

	DL	DV	DL-DV
Basis set 101			
SE	8.35	5.61	6.76
RPA	7.16	6.66	6.90
SOPPA	7.60	7.68	7.63
Basis set 105			
SE	8.35	5.54	6.72
RPA	7.04	6.93	6.98
SOPPA	7.73	7.72	7.72
Theory			
RPA[a]	7.0420	7.0128	
DOSD[b,c]	7.316		
Experiment (total spectrum)			
Photoabsorption[d]	7.12		
EMS[d]	7.22		
Experiment (continuum only, $\omega > 12.62$ eV)			
Photoabsorption[d]	6.332		
Photoabsorption and EMS[e]	5.86		
Electron impact	6.36[f]		
	6.48±0.30[g]		
Proton impact[h]	5.86		

[a]Reference 65.
[b]Dipole oscillator strength distribution (DOSD) constructed from experimental and theoretical information, empirical increment rules, etc.
[c]Reference 73.
[d]Reference 3.
[e]Reference 2.
[f]Reference 74.
[g]Reference 75.
[h]Reference 76.

TABLE V. Average static electric dipole polarizability $\bar{\alpha}=s(-2)$ for the water molecule in the dipole-length (DL), dipole-velocity (DV), and mixed (DL-DV) approximation (in a.u.). Values of the individual components of the α tensor are reported in Ref. 44.

	DL	DV	DL-DV
Basis set 101			
SE	9.64	6.92	8.05
RPA	8.50	7.83	8.14
SOPPA	10.44	11.04	10.72
Basis set 105			
SE	9.66	6.85	8.02
RPA	8.53	8.43	8.48
SOPPA	10.79	11.32	11.04
Theory			
CHF[a]	8.53		
SDTQ-MBPT(4)[a]	9.92		
SDTQ-MBPT(4)+vibr. corr.[a,b]	9.97		
Experiment			
Photoabsorption[c]	9.45		
EMS[c]	9.72		
Rayleigh depolarization[d]	9.922		

[a]Reference 69.
[b]Reference 70.
[c]Reference 3.
[d]Reference 68.

overestimated by SOPPA. This overestimation can be traced to a number of low excitation energies that come out too small in SOPPA. These observations also hold for the individual components of the dipole polarizability, which are discussed in more detail in Ref. 44.

Known moments are generally equally well reproduced by both basis sets. This is true for both RPA and SOPPA calculations. Although the agreement between moments

TABLE VI. Mean excitation energy 27.211 $I(0)$ for the water molecule in the dipole-length (DL), dipole-velocity (DV), and mixed (DL-DV) approximation (in eV).

	DL	DV	DL-DV
Basis set 101			
SE	69.77	83.01	76.19
RPA	71.98	75.38	73.71
SOPPA	71.46	69.82	70.66
Basis set 105			
SE	68.07	81.62	74.57
RPA	71.24	71.82	71.53
SOPPA	68.08	68.10	68.13
Theory			
RPA[a]	72.9151	73.0970	
DOSD[b,c]	71.62		

[a]Reference 65.
[b]Dipole oscillator strength distribution (DOSD) constructed from experimental and theoretical information, empirical increment rules, etc.
[c]References 77 and 78.

calculated in different gauges is very good, the dipole-length formulation seems to give the most reliable results. For that reason all photoionization cross sections reported in this work are calculated in this approximation.

VII. PHOTOIONIZATION CROSS SECTIONS

A. Partial cross sections of the valence-shell orbitals

In the one-electron model the ground state of the water molecule has the following orbital configuration:

$$(1a_1)^2(2a_1)^2(1b_2)^2(3a_1)^2(1b_1)^2 .$$

The five orbitals give rise to the ionization potentials 539.7, 32.2, 18.55, 14.73, and 12.62 eV, respectively.[71,72] The $1a_1$ orbital forms the inner shell, the $2a_1$ orbital the inner valence shell, and the remaining three orbitals the outer valence shell.

The partial cross sections of the valence-shell orbitals are shown in Figs. 1–4. They are calculated by the SOPPA method employing basis set 101. Cross sections obtained by the simpler RPA method are generally quite close to the SOPPA results. The SE cross sections, on the other hand, resemble more the SE results reported previously,[27–29] i.e., they tend to be far too large. The figures also show the contributions of the three polarization directions. For comparison cross sections of Tan et al.[4] obtained by electron momentum spectroscopy (EMS) are also displayed. These have been obtained for the energy range from 16 to 60 eV. Recently the data have been supplemented by a synchrotron radiation study for photon energies between 30 and 140 eV.[9] In the overlapping region the two sets of data agree very well. The low-energy and (<20 eV) of the cross sections is less certain. This is partly due to presence of narrow resonances and autoionizing states in this region.[79] On the other hand, there are considerable technical difficulties in obtaining experimentally the low-energy photoionization cross sections.[6]

Figure 1 shows the partial cross section for the non-bonding orbital $1b_1$. The cross section passes through a maximum at 18.5 eV, which is in remarkable agreement with the experimental cross section. The previous SE calculations yield a much smaller cross section in this area below 22 eV.[28,29] A more recent EMS study of this region[6] finds an even larger cross section at low energies, while synchrotron radiation measurements scatter between 4.5 and 10 Mb.[5,13] A compilation of cross sections for this orbital obtained by different methods is given in Ref. 6.

The partial cross section for the bonding orbital $3a_1$ is displayed in Fig. 2. It also agrees very well with the EMS data and shows a maximum at 19 eV which was also present in the earlier SE calculations.[27–29] Diercksen et al.[28] have suggested that it is caused by coupling between the $3a_1 \rightarrow 2b_2$ valence excitation and the $3a_1 \rightarrow kb_2$ ionization. In the present calculation a weak mixing of this excitation and the ionization channel is also observed. Again, there is considerable spread among the experimental cross sections between 18 and 22 eV. The minimum at 20 eV found in one of the experimental stud-
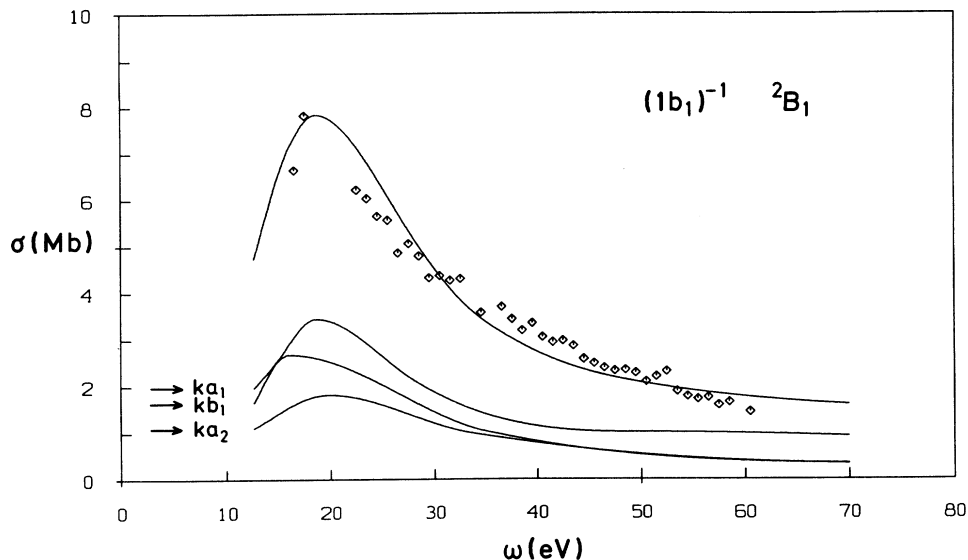
FIG. 1. Partial photoionization cross section of the $1b_1$ orbital of the water molecule (separated-channel approximation, SOPPA, basis set 101), contributions of the individual polarization directions, and experimental (EMS) reference data (Ref. 4).

ies[5] does not appear in the present calculation.

In the case of the $1b_2$ orbital the theoretical partial cross section does not agree as well with the experimental data as for the other outer valence orbitals. It lies about 1.5 Mb above the experimental points. The previous SE calculations[27-29] also show this feature. However, in the SE calculations it is much more pronounced, the cross sections becoming as large as 13 Mb. This behavior is partly reduced by a better description of the electron correlation in SOPPA. However, the fact that part of the overestimation of the cross section persists at the SOPPA level supports the suggestion of Diercksen et al.[28] that it

may be partly attributed to the neglect of channel coupling in the calculation of partial cross sections. In fact, the inclusion of channel coupling in the calculation of the total cross section has a dramatic effect in this energy region (Sec. VII B). It is interesting to note that for this partial cross section the best agreement with experiment is obtained by a scattered-wave calculation[18] whereas the scattered-wave cross sections are generally too low for the other channels.

The partial cross section of the inner valence orbital $2a_1$ is almost an order of magnitude smaller than those of the outer valence orbitals, which reflects the relative
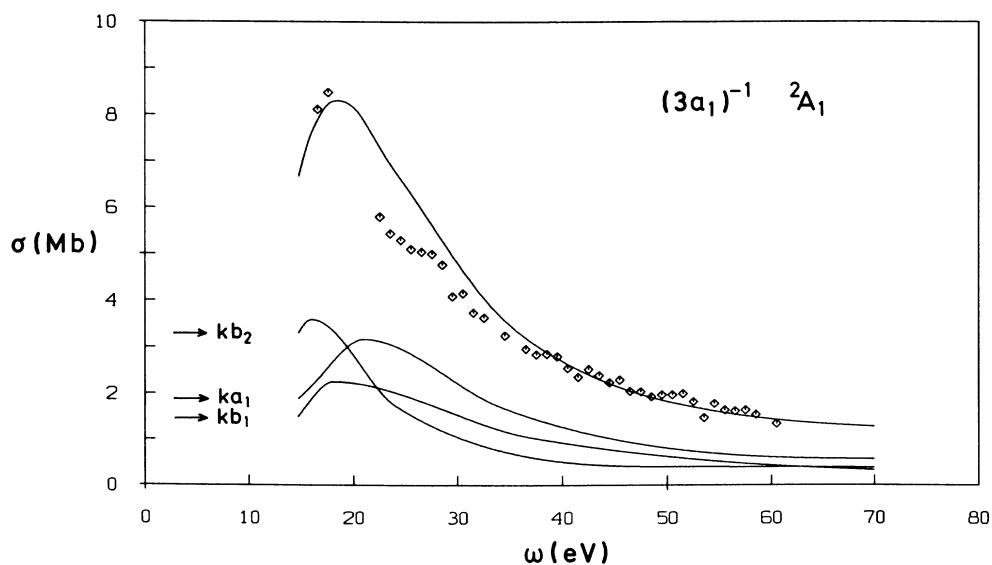
FIG. 2. Partial photoionization cross section of the $3a_1$ orbital of the water molecule (separated-channel approximation, SOPPA, basis set 101), contributions of the individual polarization directions, and experimental (EMS) reference data (Ref. 4).
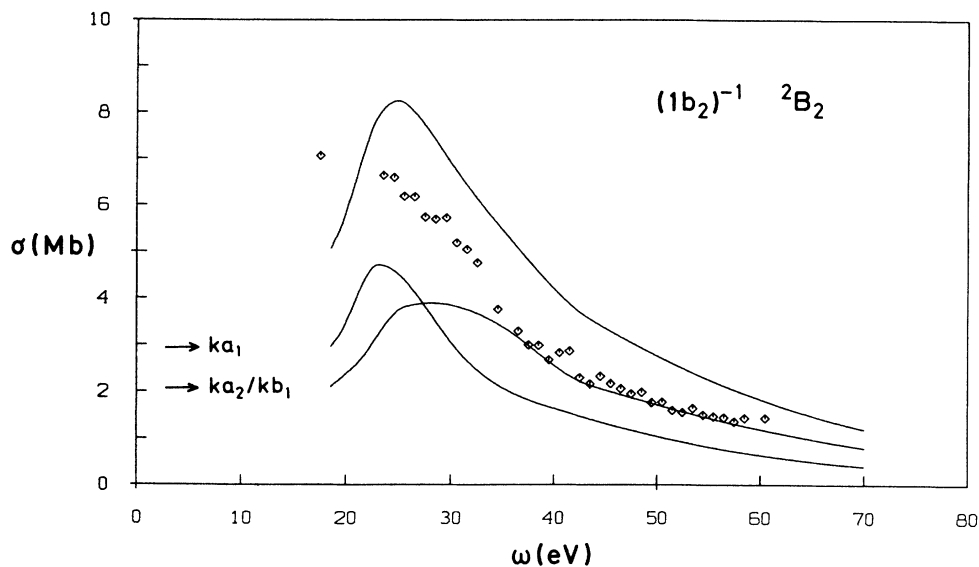
FIG. 3. Partial photoionization cross section of the $1b_2$ orbital of the water molecule (separated-channel approximation, SOPPA, basis set 101), contributions of the individual polarization directions, and experimental (EMS) reference data (Ref. 4).

compactness of this orbital. In contrast to ionization from the outer valence orbitals the SOPPA method does not give sufficient flexibility to the wave function to account fully for the orbital relaxation upon removal of an inner valence-shell electron. Therefore, the error in the ionization potential produced by the Koopmans approximation persists at the SOPPA level. On the other hand, it may be assumed to a good approximation that the Koopmans error is nearly constant for all final continuum states. Hence it is justified to shift the ionization curve of this orbital back by the Koopmans error of 4.6

eV as is done with the cross section in Fig. 4. This cross section again shows very good agreement with the EMS data[4] and also with more recent synchrotron radiation measurements[7] (marked as $\triangle$ in Fig. 4). The latter show a smaller scatter than the EMS cross sections. A comparison of several previous experimental and theoretical cross sections of this orbital can be found in Ref. 7. It shows that the previous SE results[27-29] are not quite as good as the present SOPPA calculation, while the scattered-wave[18] calculation underestimates this cross section considerably.
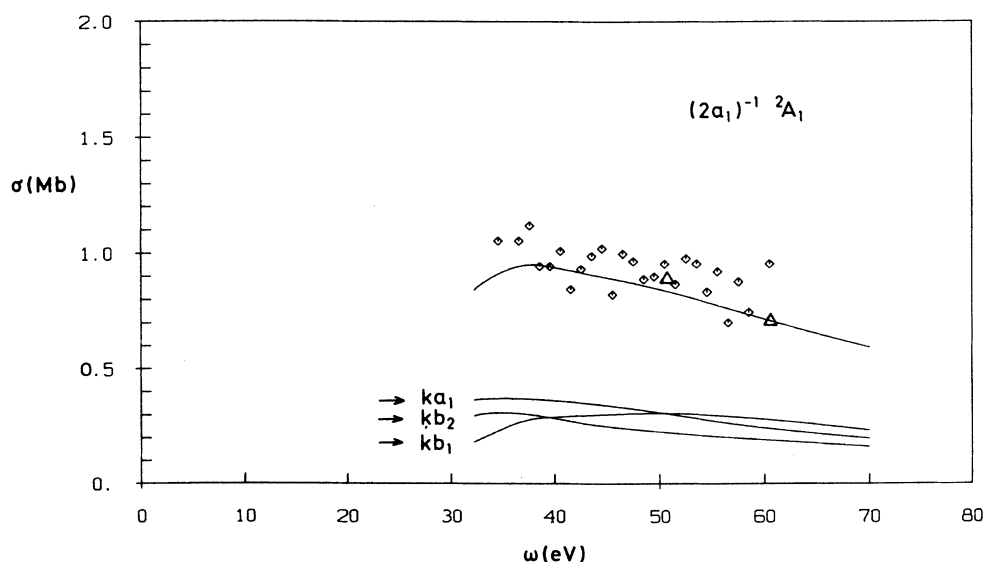
FIG. 4. Partial photoionization cross section of the $2a_1$ orbital of the water molecule (separated-channel approximation, SOPPA, basis set 101), contributions of the individual polarization directions, and experimental (EMS) reference data (Ref. 4).

B. Total valence-shell photoionization cross section

The calculation of the total valence cross section of the water molecule poses additional technical problems not encountered in the calculation of partial cross sections of single orbitals. For a complete description including channel coupling one would ideally like to include all possible single particle-hole excitations from all valence orbitals into the polarization propagator determination of the transition energies and oscillator strengths. This is feasible in RPA while for the SOPPA cross sections a partitioning of the excitation space as discussed in Sec. V has to be performed.

Another problem arises in the treatment of quasi-discrete states embedded in the ionization continuum. Excitation into a low-lying quasidiscrete state does not necessarily lead to ionization of the molecule, since it may decay into the ground state by fluorescence or may lead to dissociation of the molecule into neutral fragments. Hence, their oscillator strength does not (or at least not fully) contribute to the molecular photoionization cross section. This has been observed experimentally for energies below 20 eV, where the absorption cross section is larger than the ionization cross section.[2] Above 20 eV every absorption leads to ionization of the system. In a moment-theoretical calculation it is necessary to sort the transitions into those which correspond to quasi-discrete states and those which describe the continuum. In the present work the contributions from the individual channels to the transitions are examined and the following rule is adopted. If a transition's dominant contribution arises from a channel whose experimental ionization potential is exceeded by the transition energy then this transition is regarded as ionization and is kept in the moment-theoretical analysis. Otherwise it is regarded as transition to a quasidiscrete state and is discarded. Above 20 eV all transitions are kept. This approach to the photoionization in the low-energy regime is rather simplistic but works well for the water molecule. It is presently the only viable path since no detailed studies of the fluorescence, dissociation, and autoionization dynamics of all these resonant states have been performed. Only very recently has a quantitative theoretical description of the dynamics of the first bound excited state of water been achieved.[80] As in the case of the partial cross sections the transitions from the $2a_1$ inner valence-shell orbital are shifted to correct for the neglect of orbital relaxation. Given that the contribution of this orbital to the total cross section is quite small the shifting causes only a minor change in the total cross section.

The theoretical cross sections are compared to the recent double ionization chamber measurements of Haddad and Samson.[2] These agree very well with older EMS data of Tan et al.,[4] except in the region between 20 and 40 eV where the latter suggest a cross section which is smaller by 3 Mb.

For comparison the total cross section obtained by summing up the partial cross sections of Sec. VII A is displayed in Fig. 5. This separated-channel SOPPA cross section already shows better agreement with experiment than any of the previous theoretical studies, which underlines the importance of the use of moment-conserving polarization propagator methods in connection with moment theory. However, there are still some artifacts in the cross section like the discontinuities at each ionization potential which are not observed experimentally since channel coupling smoothens the cross section in the vicinity of the ionization potentials. Furthermore, the theoretical cross section is too large between 20 and 30 eV. This overestimation can be seen to arise from too large a cross section for the $1b_2$ orbital as discussed in Sec. VII A.

The coupled-channel total cross sections of the valence shell are calculated in basis set 105 in RPA and SOPPA
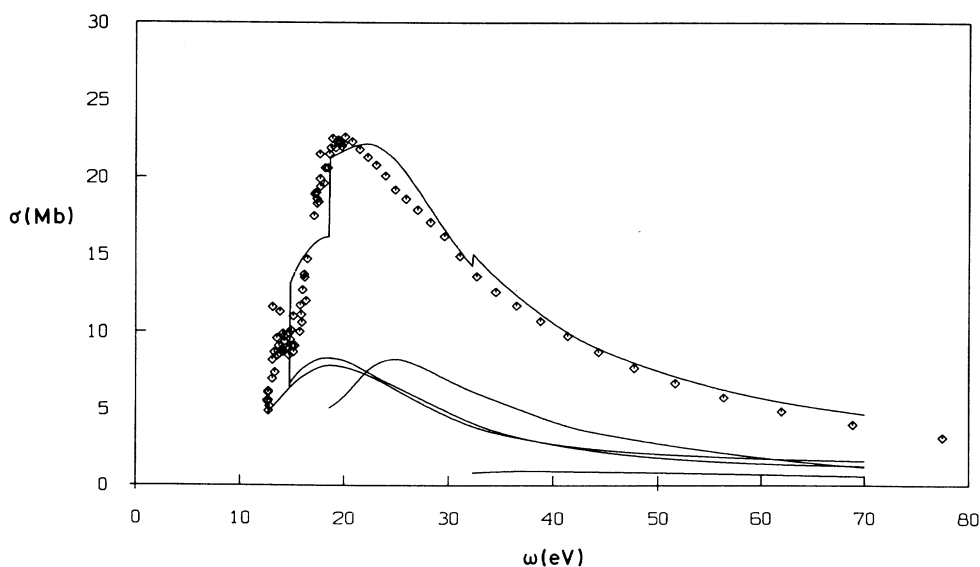
FIG. 5. Total valence-shell photoionization cross section of the water molecule calculated in the separated-channel approximation (SOPPA, basis set 101), partial contributions of the individual channels, and experimental reference data (Ref. 2).
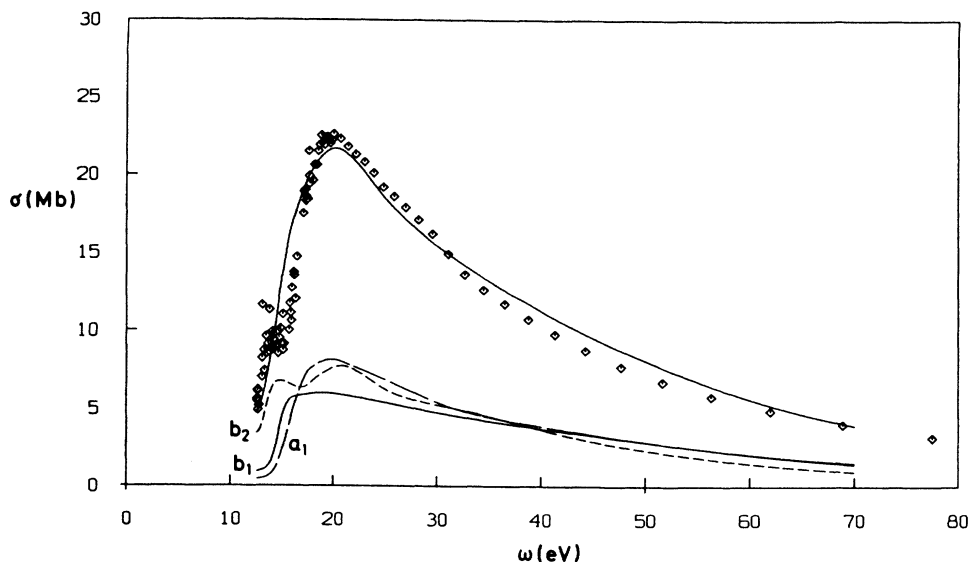
FIG. 6. Total valence-shell coupled-channel photoionization cross section of the water molecule (RPA, basis set 105), contributions of the individual polarization directions, and experimental reference data (Ref. 2).

(Figs. 6 and 7, respectively). Both approximations show by-and-large the same agreement with the experimental data. The RPA cross section approaches the experimental cross section very closely above 20 eV while it is too large at small energies. The SOPPA exhibits the opposite behavior. It perfectly matches the experiment in the energy range below the maximum, while it is too small between 20 and 30 eV.

There are various possible explanations for the marked deviation of the SOPPA curve from the experimental values above the maximum. As mentioned in Sec. VI several excitation energies come out too small in SOPPA. If this is also true for continuum transitions it would shift oscillator strength from the continuum to lower energy

regions where it is then discarded because of the energy criterion for quasidiscrete states. Most likely this behavior is caused by limitations of the second-order approach. On the other hand, it cannot be ruled out completely that the actual cross section in this area is indeed smaller than in the experiment of Haddad and Samson,[2] as is suggested by the EMS data of Tan et al.[4]

C. Inner-shell photoionization cross section

The neglect of orbital relaxation upon removal of a $1a_1$ electron has even more pronounced effects than for the $2a_1$ orbital, the error of the Koopmans approximation being 20 eV. Again, the cross section of this work is
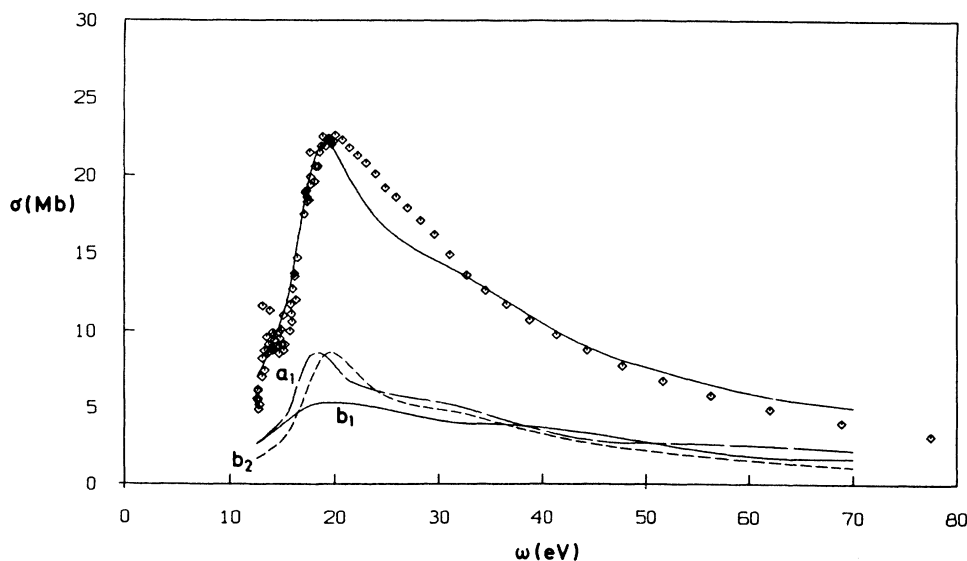
FIG. 7. Total valence-shell coupled-channel photoionization cross section of the water molecule (SOPPA, basis set 105), contributions of the individual polarization directions, and experimental reference data (Ref. 2).
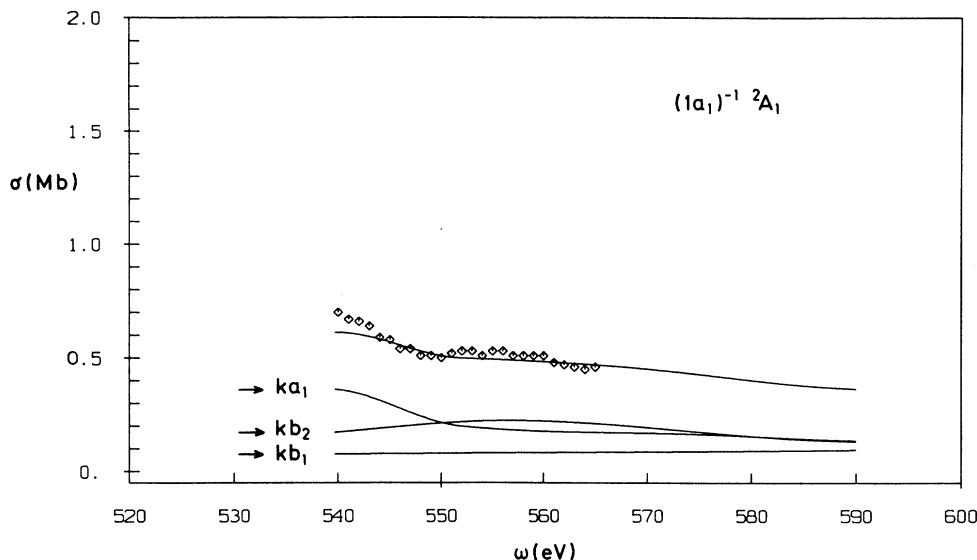
FIG. 8. Photoionization cross section of the inner-shell $1a_1$ orbital of the water molecule (separated-channel approximation, SOPPA, basis set 101), contributions of the individual polarization directions, and experimental (EMS) reference data (Ref. 8).

shifted by this amount towards smaller energies. However, it cannot be expected that this correction works as well as in the case of the inner valence-shell orbital since an inner-shell hole is a much larger perturbation. The SOPPA method can account to a small extent for this perturbation. Experience with the conceptionally related electron propagator (one-particle Green's function[81]) method, however, indicates that at least a fourth-order MBPT treatment is necessary to predict inner-shell processes reliably.[82]

Below the ionization potential of this channel four quasidiscrete states at 534.0, 535.9, 537.1, and 583.5 eV were observed in EMS studies.[8,83] These have been identified by Diercksen et al.[28] as excitations of one $1a_1$ electron into virtual valence and Rydberg orbitals. The three lower excitations are also found in the present work at 530.8, 531.4, and 535.8 eV, the fourth being too close to the continuum to be resolved. The observed disagreement between experimental and theoretical excitation energies (after Koopmans's correction) is as expected for inner-shell processes studied by a second-order method.

The cross section above the ionization potential is displayed in Fig. 8, together with reference data from a recent EMS investigation by Ishii et al.[8] which essentially reproduces older results of Wight and Brion[83] but gives absolute cross sections. Use of the recent cross section avoids the problem of renormalization of the experimental data that has been a source of arbitrariness in assessing the quality of the previous SE studies of this cross section.[28,29] The present SOPPA cross section is in remarkable agreement with the experimental results. The earlier SE calculation of Diercksen et al.[28] showed a more rapid decay of the cross section at higher energies, and the contributions of the individual excitation dipole directions to the cross section was completely different from the present cross section. The broad feature in the experimental curve at 555 eV has previously been attributed to

shake-up satellites.[28,83] It is interesting to note that the cross section of this work also shows a broad feature at 560 eV since the polarization propagator only contains single particle-hole excitations and is therefore not able to describe two-electron shake-up processes.

VIII. CONCLUSIONS

Moment-theoretical methods for the calculation of continuous photoionization cross sections rely heavily on the fact that a representation of the molecular photoionization continuum by discrete L^2 basis functions reproduces correctly the power moments of the oscillator strength in the continuum region. In this contribution various moments of the water molecule are calculated and compared to experimental and theoretical reference data. This comparison shows that the SE method is not able to reproduce known moments. It has long been known that the the SE approximation produces an error in the TRK sum rule. For the water molecule it amounts to ±20% which caused the large overestimation or underestimation of photoionization cross sections in earlier calculations.[27-29] In contrast, both RPA and SOPPA practically fulfill the TRK sum rule with the basis sets used in the present work.

In this work partial photoionization cross sections for all ground-state orbitals of the water molecule are calculated in SOPPA and fully coupled total valence-shell cross sections are calculated in RPA and SOPPA. All cross sections show better agreement with experiment than any previous calculations. It is believed that the following three reasons are responsible for this.

(i) The most important point is to use a method (and a large enough basis set) so that the TRK sum rule is effectively obeyed. This requirement rules out the SE approximation (and other incompletely CI treatments), especially since an RPA calculation is computationally

only insignificantly more expensive than an SE calculation.

(ii) The second improvement is obtained by avoiding the separated-channel approximation which causes artificial discontinuities at the ionization potentials and perhaps incorrect cross sections elsewhere. In the case of the water molecule the remaining error in the partial cross section of the $1b_2$ orbital can be explained as an effect of the separated-channel approximation.

(iii) The inclusion of electron correlation as such seems to have the smallest effect on the calculated photoionization cross section of the water molecule once conditions (i) and (ii) are met since the RPA cross sections are not much inferior to the SOPPA cross sections. This result may not be generalized to other systems. Canuto et al.[39,84] have reported a case where even higher orders than SOPPA had to be included to obtain reliable moments and cross sections. However, the success of RPA in the case of the water molecule suggests that the cross sections of much larger systems can also be reliably obtained if electron correlation is not of utmost importance.

ACKNOWLEDGMENTS

*Present address: Science and Engineering Research Council, Daresbury Laboratory, Warrington WA4 4AD, United Kingdom.

[1]R. H. Page, R. J. Larkin, Y. R. Shen, and Y. T. Lee, J. Chem. Phys. 88, 2249 (1988).

[2]G. N. Haddad and J. A. R. Samson, J. Chem. Phys. 84, 6623 (1986).

[3]J. Berkowitz, Photoabsorption, Photoionization, and Photoelectron Spectroscopy (Academic, New York, 1979).

[4]K. H. Tan, C. E. Brion, Ph. E. van der Leeuw, and M. J. van der Wiel, Chem. Phys. 29, 299 (1976).

[5]C. M. Truesdale, S. Southworth, P. H. Kobrin, D. W. Lindle, G. Thornton, and D. A. Shirley, J. Chem. Phys. 76, 860 (1982).

[6]C. E. Brion and F. Carnovale, Chem. Phys. 100, 291 (1985).

[7]C. E. Brion, D. W. Lindle, P. A. Heimann, T. A. Ferrett, M. N. Piancastelli, and D. A. Shirley, Chem. Phys. Lett. 128, 118 (1986).

[8]I. Ishii, R. McLaren, A. P. Hitchcock, and M. B. Robin, J. Chem. Phys. 87, 4344 (1987).

[9]M. S. Banna, B. H. McQuaide, R. Malutzki, and V. Schmidt, J. Chem. Phys. 84, 4739 (1986).

[10]R. Cambi, G. Ciullo, A. Sgamellotti, C. E. Brion, J. P. D. Cook, I. E. McCarthy, and E. Weigold, Chem. Phys. 91, 373 (1984).

[11]A. O. Bawagan, L. Y. Lee, K. T. Leung, and C. E. Brion, Chem. Phys. 99, 367 (1985).

[12]A. O. Bawagan, C. E. Brion, E. R. Davidson, and D. Feller, Chem. Phys. 113, 19 (1987).

[13]O. Dutuit, A. Tabche-Fouhaile, I. Nenner, H. Frohlich, and P. M. Guyon, J. Chem. Phys. 83, 584 (1985).

[14]J. W. Rabalais, T. P. Debies, J. L. Berkosky, J.-T. J. Huang, and F. O. Ellison, J. Chem. Phys. 61, 516 (1974); 61, 529 (1974).

[15]S. Iwata and S. Nagakura, Mol. Phys. 27, 425 (1974).

[16]P. R. Hilton, S. Nordholm, and N. S. Hush, Chem. Phys. Lett. 64, 515 (1979).

[17]D. A. Kilcoyne, C. M. McCarthy, S. Nordholm, N. S. Hush, and P. R. Hilton, J. Electron Spectrosc. 36, 153 (1985).

[18]M. Roche, D. R. Salahub, and R. P. Messmer, J. Electron Spectrosc. 19, 273 (1980).

[19]J. Tennyson, C. J. Noble, and P. G. Burke, Int. J. Quantum Chem. 29, 1033 (1986).

[20]J. A. Richards and F. P. Larkins, J. Phys. B 17, 1015 (1984).

[21]L. A. Collins and B. Schneider, Phys. Rev. A 29, 1695 (1986).

[22]R. R. Lucchese and V. McKoy, Phys. Rev. A 24, 770 (1981).

[23]J. A. Stephens and V. McKoy, J. Chem. Phys. 88, 1737 (1988).

[24]C. T. Corcoran and P. W. Langhoff, J. Math. Phys. 18, 651 (1977).

[25]P. W. Langhoff, in Electron-Molecule and Photon-Molecule Collisions, edited by T. Rescigno, V. McKoy, and B. Schneider (Plenum, New York, 1979).

[26]G. R. J. Williams and P. W. Langhoff, Chem. Phys. Lett. 60, 201 (1979).

[27]J. J. Delaney, V. R. Saunders, and I. H. Hillier, J. Phys. B 14, 819 (1981).

[28]G. H. F. Diercksen, W. P. Kraemer, T. N. Rescigno, B. V. McKoy, S. R. Langhoff, and P. W. Langhoff, J. Chem. Phys. 76, 1043 (1982).

[29]I. Cacelli, R. Moccia, and V. Carravetta, Chem. Phys. Lett. 90, 313 (1984).

[30]P. W. Langhoff, S. R. Langhoff, T. N. Rescigno, J. Schirmer, L. S. Cederbaum, W. Domcke, and W. von Niessen, Chem. Phys. 58, 71 (1981).

[31]P. W. Langhoff, in Electron-Atom and Electron-Molecule Collision, edited by J. Hinze (Plenum, New York, 1983).

[32]R. F. Stewart, C. Laughlin, and G. A. Victor, Chem. Phys. Lett. 29, 353 (1974).

[33]G. R. J. Williams and P. W. Langhoff, Chem. Phys. Lett. 78, 21 (1981).

[34]A. P. Hitchcock, C. E. Brion, G. R. J. Williams, and P. W. Langhoff, Chem. Phys. 66, 435 (1982).

[35]A. P. Hitchcock, G. R. J. Williams, C. E. Brion, and P. W. Langhoff, Chem. Phys. 88, 65 (1984).

[36]I. Cacelli, V. Carravetta, and R. Moccia, Mol. Phys. 59, 385 (1986).

[37]I. Cacelli, V. Carravetta, and R. Moccia, Chem. Phys. 120, 51 (1988).

[38]P. Swanstrøm, J. T. Golab, D. L. Yeager, and J. A. Nichols, Chem. Phys. 110, 339 (1986).

[39]S. Canuto, J. Geertsen, F. Müller-Plathe, and G. E. Scuseria, J. Phys. B 21, 3891 (1988).

[40]J. Oddershede, Adv. Chem. Phys. 69, 201 (1987).

[41]U. Fano and J. W. Cooper, Rev. Mod. Phys. 40, 441 (1968).

[42]H. A. Bethe and E. E. Salpeter, Quantum Mechanics of One- and Two-Electron Atoms (Springer, Berlin, 1957; reprinted by Plenum, New York, 1977).

[43]J. A. Shohat and J. D. Tamarkin, The Problem of Moments (American Mathematical Society, Providence, 1943).

[44]F. Müller-Plathe, Ph.D. thesis, Technische Universität,

München, 1988; Institut für Astrophysik, Garching, Report No. 368, 1988.

[45]P. J. Davis and P. Rabinowitz, *Methods of Numerical Integration*, 2nd ed. (Academic, Orlando, 1984).

[46]C. Blumstein and J. C. Wheeler, Phys. Rev. B **8**, 1764 (1973).

[47]H. S. Wall, *Analytic Theory of Continued Fractions* (Van Nostrand, New York, 1948; reprinted by Chelsea, New York, 1973).

[48]P. W. Langhoff, C. T. Corcoran, J. S. Sims, F. Weinhold, and R. M. Glover, Phys. Rev. A **14**, 1042 (1976).

[49]J. M. Hyman, SIAM J. Sci. Stat. Comput. **4**, 645 (1983).

[50]G. Szegö, *Orthogonal Polynomials*, 4th ed. (American Mathematical Society, Providence, 1975).

[51]R. Moccia (private communication).

[52]J. O. Hirschfelder, W. Byers Brown, and S. O. Epstein, Adv. Quantum Chem. **1**, 255 (1964).

[53]H. A. Bethe, Ann. Phys. (Leipzig) **5**, 325 (1930).

[54]M. Inokuti, Rev. Mod. Phys. **43**, 297 (1971).

[55]H. A. Bethe and R. Jackiw, *Intermediate Quantum Mechanics*, 3rd ed. (Cummings, Menlo Park, 1986).

[56]J. Oddershede, Adv. Quant. Chem. **11**, 275 (1978).

[57]J. Oddershede, P. Jørgensen, and D. L. Yeager, Comput. Phys. Rep. **2**, 33 (1984).

[58]J. Geertsen, Adv. Quantum Chem. (to be published).

[59]A. E. Hansen, Mol. Phys. **13**, 425 (1967).

[60]P. Jørgensen, J. Oddershede, and N. H. F. Beebe, J. Chem. Phys. **68**, 2527 (1978).

[61]A. J. Sadlej, in *Proceedings of the 7th Seminar on Computational Methods in Quantum Chemistry*, edited by B. T. Sutcliffe (University of York, York, 1987); Int. J. Quantum Chem. **35**, 409 (1989).

[62]P. Jørgensen and J. Oddershede, J. Chem. Phys. **78**, 1898 (1983).

[63]J. Oddershede and P. Jørgensen, J. Chem. Phys. **66**, 1541 (1977).

[64]P. Lazzeretti and R. Zanasi, J. Chem. Phys. **83**, 1218 (1985).

[65]J. Geertsen, J. Oddershede, and J. R. Sabin, Phys. Rev. A **34**, 1104 (1986); the moments reported in this article have been calculated at the RPA level using basis set 101 and should hence be equal to the corresponding results of the present work and of Ref. 64. The deviations are due to the use of different convergence thresholds in various parts of the calculation. By applying more stringent conditions Oddershede and Sabin have achieved perfect agreement with the results of Ref. 64. Here, their corrected values for $s(0)$, $s(-1)$, and $I(0)$ are listed [J. Oddershede and J. R. Sabin (private communication)]. This point is only of technical interest and does not affect the conclusions of their work.

[66]G. H. F. Diercksen, N. E. Grüner, and J. Oddershede, Comput. Phys. Commun. **30**, 349 (1983).

[67]G. H. F. Diercksen and W. P. Kraemer, MUNICH Reference Manual (Max-Planck-Institut für Physik und Astrophysik, München, 1981).

[68]W. F. Murphy, J. Chem. Phys. **67**, 5877 (1977).

[69]G. H. F. Diercksen, V. Kellö, and A. J. Sadlej, J. Chem. Phys. **79**, 2918 (1983).

[70]G. D. Purvis III and R. J. Bartlett, Phys. Rev. A **23**, 1594 (1981).

[71]K. Siegbahn, C. Nordling, G. Johansson, J. Hedman, P. F. Heden, K. Hamrin, U. Gelius, T. Bergmark, L. O. Werme, R. Manne, and Y. Bauer, *ESCA Applied to Free Molecules* (North-Holland, Amsterdam, 1969).

[72]D. W. Turner, C. Baker, A. D. Baker, and C. R. Brundle, *Molecular Photoelectron Spectroscopy* (Wiley, New York, 1970).

[73]G. D. Zeiss, W. J. Meath, J. C. F. MacDonald, and D. J. Dawson, Can. J. Phys. **55**, 2080 (1977).

[74]J. Schutten, F. J. de Heer, H. R. Moustafa, A. J. H. Boerboom, and J. Kistemaker, J. Chem. Phys. **44**, 3924 (1966).

[75]F. F. Rieke and W. Prepejchal, Phys. Rev. A **6**, 1507 (1972).

[76]M. E. Rudd, T. V. Goffe, R. D. DuBois, and L. H. Toburen, Phys. Rev. A **31**, 492 (1985).

[77]G. D. Zeiss, W. J. Meath, J. C. F. MacDonald, and D. J. Dawson, Rad. Res. **70**, 284 (1977).

[78]International Commission on Radiation Units and Measurements, Bethesda, Report No. 37, 1984.

[79]P. Gürtler, V. Saile, and E. E. Koch, Chem. Phys. Lett. **51**, 386 (1977).

[80]V. Engel, R. Schinke, and V. Staemmler, J. Chem. Phys. **88**, 129 (1988).

[81]W. von Niessen, J. Schirmer, and L. S. Cederbaum, Comput. Phys. Rep. **1**, 57 (1984).

[82]G. Angonoa, O. Walter, and J. Schirmer, J. Chem. Phys. **87**, 6789 (1987).

[83]G. R. Wight and C. E. Brion, J. Electron Spectrosc. **4**, 25 (1974).

[84]S. Canuto, W. Duch, J. Geertsen, F. Müller-Plathe, J. Oddershede, and G. E. Scuseria, Chem. Phys. Lett. **147**, 435 (1988).